Acoustic Trilateration Monitoring for Laser Surface Processing

Clovis Alleaume*, Iago Camaño Lagoa, Camilo Prieto Río,
Sara Vidal Álvarez, and Jaime Cuartero Del Pozo

AIMEN Centro Tecnológico – O Porriño, Spain
**Corresponding author's e-mail: clovis.alleaume@aimen.es*

As the laser processing industry grows bigger every year, the need for process monitoring grows with it. To this extent, in this paper, we will present a new and innovative way to monitor the spatial accuracy of laser processing based on acoustic monitoring and multilateration of the soundwave emitted during the laser-material interaction. During laser surface processing, the interaction of the laser with the material's surface emits a soundwave. By placing an array of various acoustic sensors surrounding the processing area, one can measure the difference in Time-of-Flight of the shockwave that is emitted by the laser ablation. Once this time difference is measured, it becomes possible to locate the origin of the sound with sub-millimeter accuracy. The marking of a QR code by a ns pulsed laser will be used to showcase the viability of this method. The real location of the surface marking process will be compared with the location obtained in-line with the acoustic trilateration monitoring. After demonstrating this new method, we will discuss its potential applications for the laser processing industry, the limitations it suffers, and how those issues could be mitigated or overcome.

DOI: 10.2961/jlmn.2024.03.2008
Keywords: laser processing, surface texturing, acoustic emission, multilateration, trilateration, triangulation, process monitoring

1. Introduction

As laser surface processing becomes easily accessible [1], it becomes increasingly used by industrials for various applications such as surface texturing or selective ablation/laser cleaning [2]. Numerous processing machines can be found on the market, and every year, the quality of the laser processes increases, thanks to better laser systems hardware, better monitoring, control, and inspection systems

Monitoring the process has become a vital element for first-time-right and zero-defect manufacturing, and in-line, real-time in-situ monitoring methods are paramount for high yield high throughput systems [3][4].

To this extent, a new monitoring setup was created at AIMEN within the BILASURF European project, allowing us to validate our system output in-line. This project aims at developing and integrating a process for high-rate laser functionalization of complex 3D surfaces using tailored designed riblets to reduce friction. Metallic surfaces are texturized by means of a galvanometric scanner directing a 1064nm ps laser toward the sample mounted onto a robotic arm.

Previous work on acoustic monitoring in pulsed laser material processing focused on the study of characteristic signals to determine process focal position or to monitor certain operating conditions. [5-8] In this work, in order to ensure that the laser interact with the sample at the predetermined location in space, an innovative setup based on an array of free space microphones is used to calculate the position of the sound emitted by the interaction laser-material based on pseudo-range multilateration algorithms.

This paper will present this new technique along with its advantages and limitations. To measure and demonstrate the adequacy of said technique, a more traditional texturization routine will be used, where a QR code is marked on an anodized aluminum surface by a laser scanner system, and the obtained results will be presented. The location calculated by the multilateration algorithm will be compared with the known location of the laser pulse, and we will demonstrate that a sub-millimeter accuracy is obtained in real time with this new method.

This acoustic monitoring setup is fully independent from the laser-scanner system. This means that no information whatsoever is gathered at system laser (no laser trigger, no known position of the scanner…), and we will present new means of obtaining those values independently. We chose this approach as it is the hardest, and from there is much easier to improve accuracy by gathering information from the system (especially the laser trigger). This also allows our system to be easily implemented in any laser system, regardless of its connectivity.

To understand this new method of measuring the position in space of the interaction between the laser and the sample, one can look at Figure 1, where the schematic of the experiment is described. As we can see, when the laser pulse hits the sample, a soundwave is produced and is propagated in free space around the sample in a spherical shockwave. The array of microphones located around the sample will capture this soundwave at different moments in time based on their relative distance from the sound origine. This difference of arrival of the sound wave is called Time Difference of Arrival, or TDoA, and since the microphones are fixed, only changes when the origine of the sound moves in space.

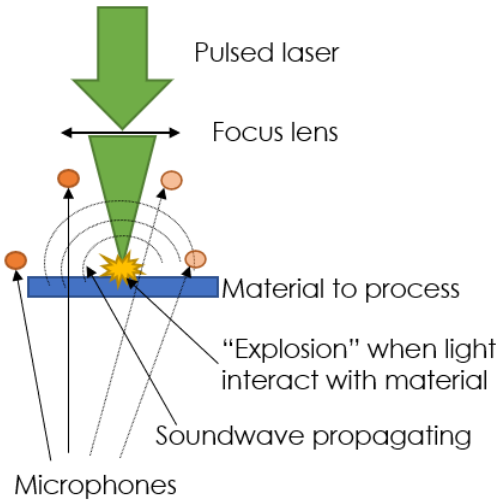

Fig. 1 Multilateration principle based on soundwave propagation in free space.

2. Experimental setup

To test our new approach to monitor the laser texturing, a known setup was used, as this allows us to easily compare the results obtained with known coordinates.

Therefore, a Coherent-Rofin industrial marking system CombiLine was used. The main wavelength of 1064nm was used, with laser pulses of 10ns. Each pulse carries 0.6mJ of energy, with a repetition rate of 20kHz. The system is equipped with a galvanometric scanner with a f-theta lens of 255mm focal, and a motorized gantry system for sample positioning. The system can be seen in Figure 3.

A sample of anodized aluminum is placed under the laser scanner system, and an array of 4 free-field microphones are placed around the area to be texturized. The microphones are models 146AE ½" free field from GRAS, and are rated for a frequency of up to 20kHz. The setup can be visible on the Figure 2.

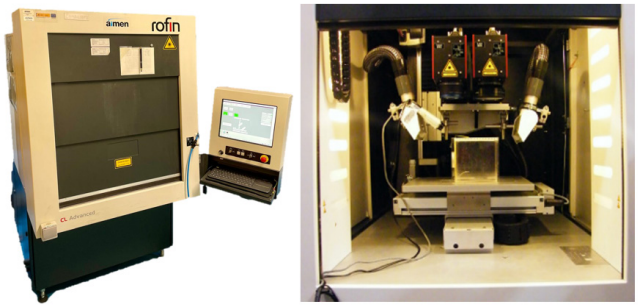

Fig. 2 Laser system used for the experimental setup: combi-line from Rofin, with laser scanner and gantry system.

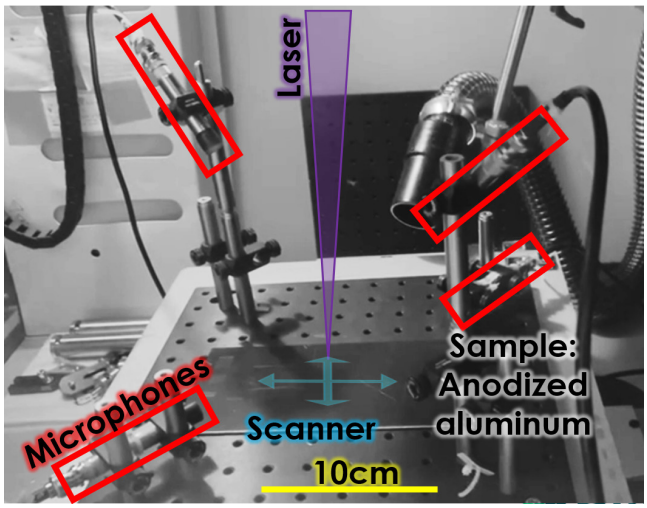

Fig. 3 Experimental setup placed inside the combiline: an array of free-filed microphones are placed below the scanner around the sample.

The four microphones are connected to a data acquisition device (DAQ) type Picoscope, that captures the voltages produced by the piezoelectric microphones at a frequency of 2Mhz. The DAQ is connected to a dedicated computer, that capture the data in real time, clean them with different algorithms and process them. A low pass filter with very high frequency (between 40kHz and 200kHz depending on the application) is used to smooth the data and remove the electrical noise, and a high pass filter is applied (400Hz) to remove the background noise. Additionally, a dedicated filter can be used to remove the specific frequency due to the extraction system (system dependent).

3. Principle, soundwave and TDoA

In the case of a single pulse, the soundwave that reaches the microphone is very easily understandable as we can see in Figure 4. The laser pulse produces a single peak of acoustic energy (AE) that can easily be identified. Various algorithms can then be used to measure the difference in the time of arrival based on peak detection or on correlation.

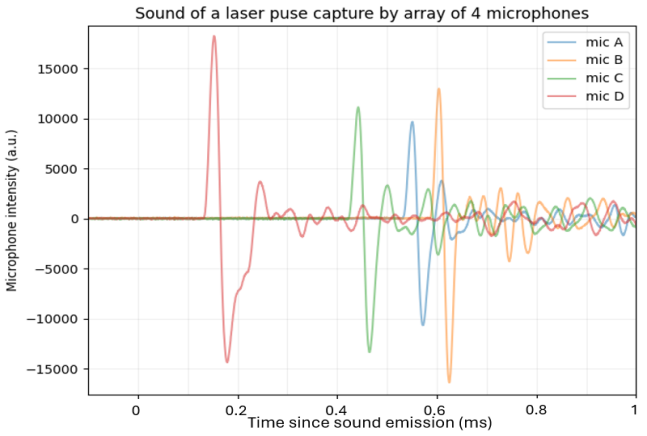

Fig. 4 Sound (acoustic energy) of a single laser pulse as captured by an array of 4 microphones.

However, things get more complicated when the laser is no longer used in single pulse mode but in burst mode or continuous mode. In both cases, a train of pulses will be applied to the sample, and due to the very high frequency of the laser and the slow speed of sound, it is very likely that the sound of the pulse n reaches the further microphone after the sound of the pulse n+1 reached the closest microphone. To solve this problem, it becomes necessary to index all registered pulses within the pulse train to compare their respective time of arrival. This interlacing of time of arrival of the sound wave and the pulse indexation can be visible in Figure 5.

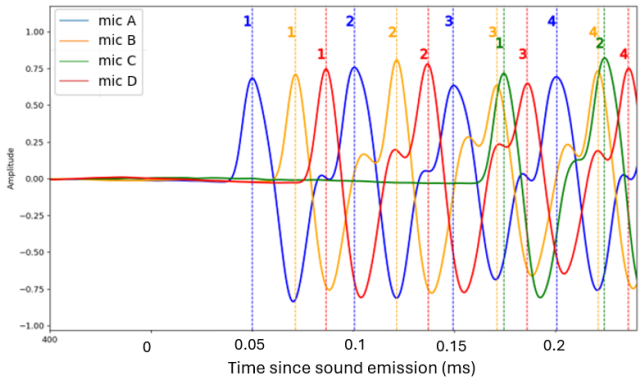

Fig. 5 Sound emission of a train of laser pulse, and indexation of each laser pulse along the train.

Another approach consists of considering the whole train at once, and perform a swiping correlation calculus, to match the signals and therefore calculated their TDoA.

TDoA are calculated based on a "master" channel, in our case channel A. This means that for 4 microphones, 3 TDoA are obtained. Once the TDoAs between the microphones are obtained, it becomes possible to calculate the position and the timing of the origin of the sound by applying a pseudo-range multilateration algorithm. Figure 6 illustrates this notion for a better understanding of the problem.

Additionally, it is possible when a train of pulses is used to perform the correlation between the 4 channels over the entire train. For example, to print a pixel of our application, 21 parallel lines with each 5 laser pulses are used. To accelerate the calculation, we can correlate the measurement over each line.

4. Multilateration

The problem we try to solve is a pseudo-range multilateration problem. This means that we try to do a lateration (find the position of the emitter in space based on the length between the emitter and the receptors; not to be confused with triangulation that based the calculus on angle measurement) on more than 3 receptors (so multi instead of trilateration, although the term trilateration is also commonly used). It is pseudo-range which means we do not know the time of emission, although this time is the time of the laser and could be gathered by monitoring the laser trigger, in this work the choice was made to not get this information to make the setup fully independent of the system, allowing us for better retrofitting on any laser machine.

Numerous algorithms exist for pseudo-range multilateration [9-12]. But for all pseudo-range multilateration algorithms, the concept is that the Times of Arrival (TOA) are measures (and their differences computed to obtain the TDoA), but the Time of Transmission (TOT) is unknown. Notice that this TOT could be obtained by measuring the electrical trigger of the laser, but chose not to as we want this new metrology setup to be fully independent of the machine. By applying the trilateration algorithm, we will be able to determine both the position of the sound source (laser interaction with sample) along with the TOT (time when the laser hits the sample).

In this study, we decided to use the pseudo-range multilateration algorithm based on the intersection of 4 spheres. The overall idea is to draw around each microphone a sphere with a radius equal to the Time of Flight (TOF, unknown) multiplied by the speed of sound. This TOF is equal to TOA – TOT. Since TOAs are measured, all 4 spheres only posse one unknown variable, TOT. The algorithm will therefore optimize TOT to discover the value for which all 4 spheres intersect in space. Figure 6 illustrates the concept of TOT, TOF, TOA, and TDoA for a master microphone and two additional ones.

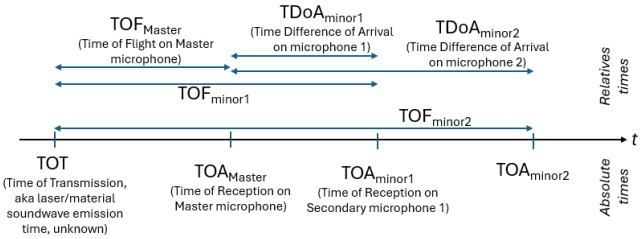

Fig. 6 Illustration of TOT (time of transmission), TOA (time of arrival), TOF (time of flight) and TDoA (time difference of arrival) for a master microphone and two secondary microphone.

To calculate this interaction point, first the intersection point of 3 spheres is calculated based on the close-form mathematical solution as presented by Fang [13]. This intersection point is a function of the positions of each microphone, which are fixed in space, and of the radius of each sphere. Since the difference in radius of each sphere is proportional to the TOF of each laser pulse, which is the sum of TOF of the master microphone and the TDoA of the current microphone and the speed of sound, the intersection for a given pulse is only a function of the TOF of the "master" microphone. The function describing the field of possible results for this interaction as a function of TOF can be represented by the interaction between two intersecting hyperboloids [14]. It becomes therefore possible to optimize this TOF in such way that the interaction point between those 3 spheres present a minimized distance with respect to the 4th sphere, aka that the distance between the interaction of the 3 spheres and center of the 4th sphere is equal to the diameter of the 4th sphere, which is equal to TOF of the master microphone plus TDoA of said 4th microphone - multiplied by the speed of sound. This way, the intersection point between the 4 spheres is calculated. The TOF of the master microphone can then be used to determinate the TOT directly as it's directly TOA of said microphone minus his TOF, and the position is space is calculated as it is the mathematical solution of the intersection of the 3 spheres for this TOF. Such result can be observed in

Figure 7, where the interaction point between the 4 spheres is shown.

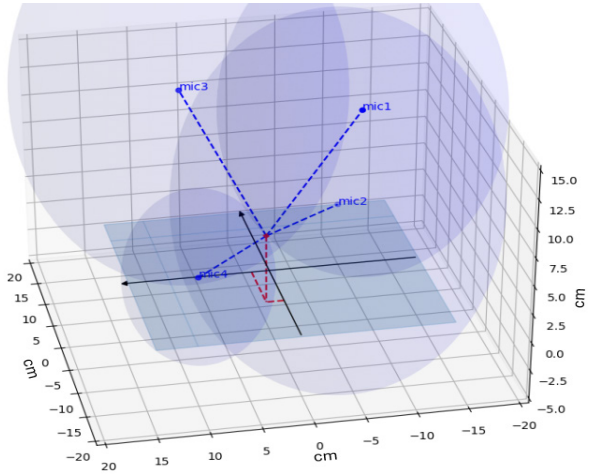

Fig. 7 Illustration of the multilateration algorithm based on the calculus of the intersection of 4 spheres of radius $(TOF_{Master} + TDoA_{Master\text{-}mic}) * v_{speed\ sound}$

This multilateration algorithm can be used on every single laser pulse or on the TDoAs times calculated for laser pulse trains as recorded during the process in an in-line process. We only need to wait for the current train to finish to be able to correctly index the pulses so the algorithm can only real-time on single pulse processes, so the algorithm is not fully real-time.

5. Application: laser printing of QR code

To validate our new monitoring setup, and before moving to an unknown machine, we used the previously presented CombiLine to process the surface of an adonized aluminum sample to mark a QR code. Each pixel of the QR code is composed of 21 lines produced by the scanner, during which 5 pulses are captured by the microphones. The QR code contain 311 pixels of 0.5x0.5 mm² placed along a 25x25 pixels matrix, creating a QR code of 12.5x12.5 mm². To print the QR code properly a double path is performed, so we register the QR processing twice.

Two approaches are used to apply the algorithm. The first approach considers each individual line of 5 pulses, that we call train of pulses, and we correlate the signal received during the line processing (so 5 pulses) to obtain the TDoAs. This way, we obtain 311*21*2 = 6.531 individual measurements per path, which each their set of TDoA. The trilateration algorithm is applied in every measurement, and the obtained position in space can be displays in a color map, where X and Y are represented and the colorscale correspond to the measured Z. The actual printed QR code can be seen in Figure 8, while the results of the multilateration algorithm are visible on Figure 9.

As one can see, the multilateration algorithm allows us to locate each train of pulses with a very good accuracy. In the zoomed-in illustration (Figure 10), the distance between the actual point and the location as obtained by the multilateration algorithm is drawn with red lines.

Fig. 8 Laser-processed sample: QR code printed onto anodized aluminum with pulsed IR laser via galvanometric scanner.

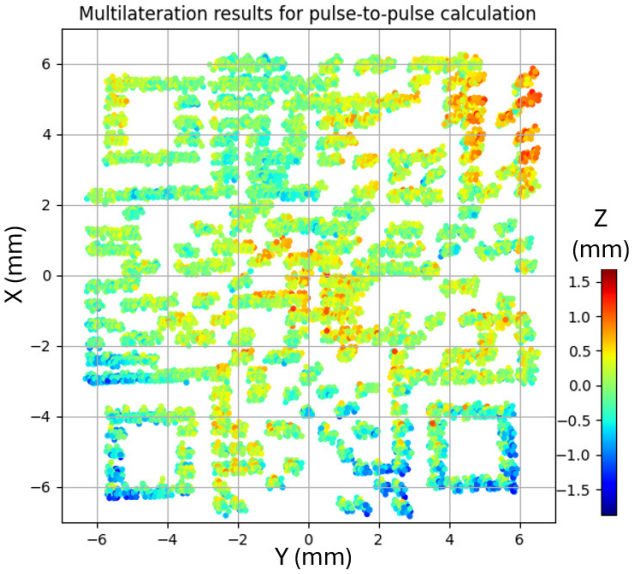

Fig. 9 Calculated location in X-Y-Z space for each train of laser pulse based on their TDoAs and pseud-range multilateration algorithm. The calculated height in Z is shown with the colorbar.

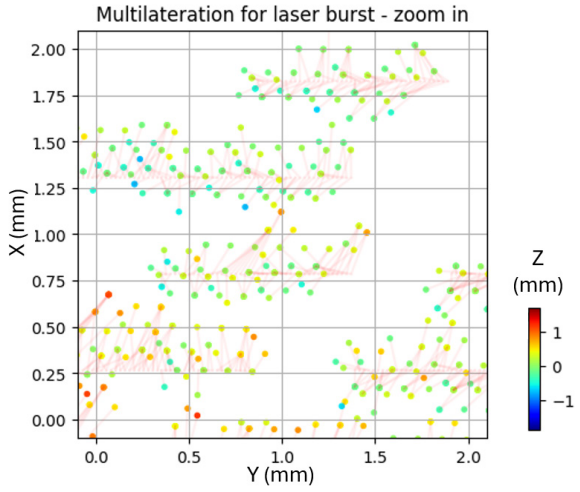

Fig. 10 Zoomed-in results of the location of the pulse as calculated by the multilateration algorithm. The difference with the actual train center location is displayed with the red lines.

It is possible to quantify this error, by plotting the distribution of this difference, and statistics such as fitting a skew gaussian can be performed. This exercise can be repeated for unidirectional distances such as vertical displacement, along the X and Y axis, and horizontal displacement (using both X & Y at once). Figure 11 shows the distribution of the position difference, and we can clearly say that our multilateration algorithm gives us results with a sub-millimeter accuracy. The Figure 12 shows the error distribution along the horizontal axis, X axis and Y axis where an error >350µm is obtained, and vertical axis where most of the error is located.

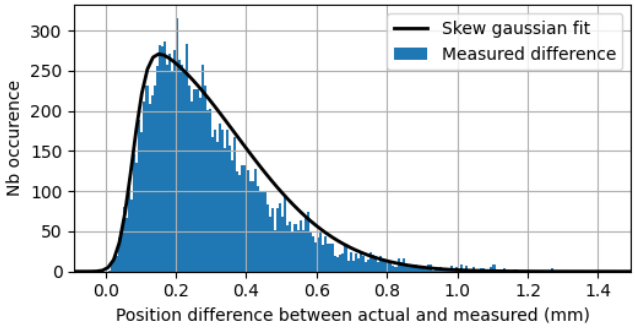

Fig. 11 Distribution of the error between the calculated position with multilateration and the actual laser position given by the laser scanning system for pulse train data.

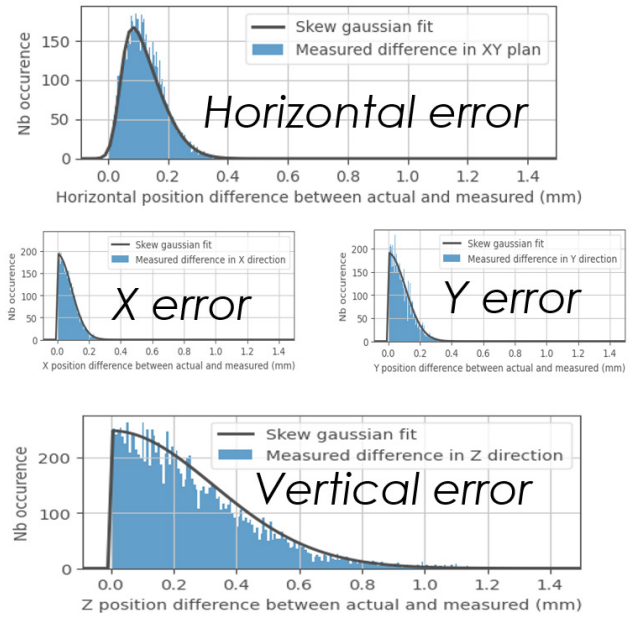

Fig. 12 Error distribution for individual dimension: the position difference between the actual and calculated position is shown as an histogram with a skew gaussian fit for horizontal (with both X & Y combined), individual X and Y error, and Z vertical error.

To finalize, we can draw a table with the different sigma value of skew gaussian fit, and the corresponding percentiles as given by the data. Those values are visible in Table 1.

Table 1 Table 1: Percentiles evolution of the position error for pulse train data and their corresponding skew normal fit sigma's.

Pulse train data	-3σ 0.1per	-2σ 0.2p	-σ 15.9p	mean 50per	σ 84.1p	2σ 97.8p	3σ 99.9p
Total error measurement	0.03	0.04	0.18	0.33	0.59	1.01	1.5
Total error skew fit	0.02	0.04	0.17	0.34	0.6	0.87	1.36
Vertical error raw data	3E-04	0.01	0.07	0.25	0.56	0.98	1.48
Horizontal error raw data	0.01	0.01	0.08	0.16	0.25	0.35	0.47
X error raw data	1E-04	3E-04	0.03	0.11	0.21	0.32	0.41
Y error raw data	1E-04	3E-04	0.03	0.08	0.16	0.28	0.41

The second approach consists of looking at each individual laser pulses. Each of the 311 pixels contains 21 lines with each 5 laser pulses, over two paths, leading to 311*21*5*2 = 65.310 measurements point. The position of the sound origine is calculated for each one of those measurements point, and in a similar manner, we can draw the map of the XY position with colorscale to represent the 3rd dimension. The overall results are displayed in Figure 13 where the calculated position of each laser pulse successfully reproduces the QR code as it is printed.

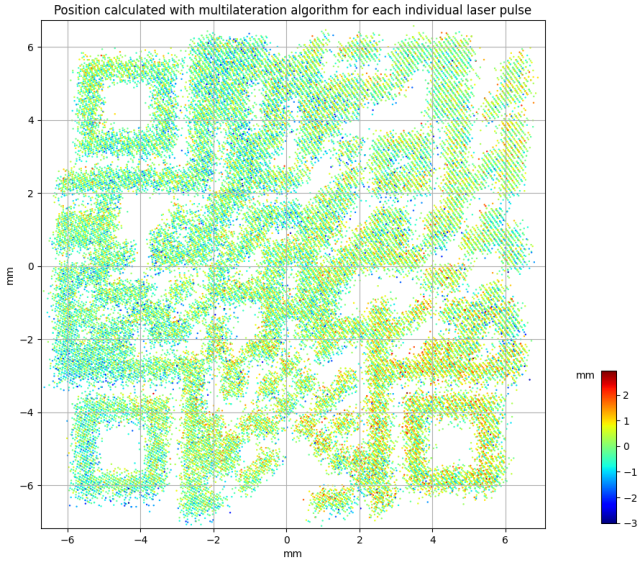

Fig. 13 Results of the multilateration algorithm position calculation for each individual pulses.

Additionally, the position error distribution can be studied in a similar way, and the results are displayed in Figure 14, and the statistical results can be compared in Table 2.

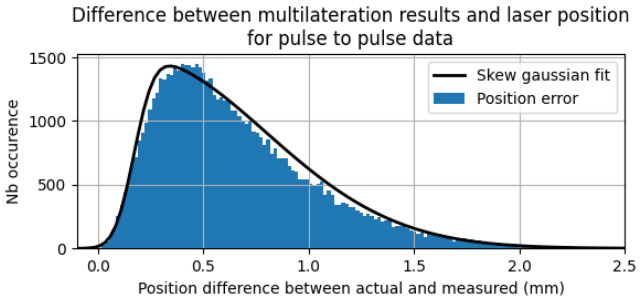

Fig. 14 Distribution of the error for pulse-to-pulse data. Compared to the pulse-train data (shown in Figure 11), the error is bigger, due to each pulse measurement having an intrinsic error in it's TDoA measurement that is not averaged as in the pulse-train TDoA calculation.

As we can observe, the pulse-to-pulse error is significantly bigger than when a pulse train is considered. This is due to the calculation of the TDoA with the pulse-to-pulse data, as each pulse measurement carries an intrinsic error. In comparison, when measuring the TDoA of a pulse train, the errors are averaged over the various pulses within the train, causing the error to diminish.

Table 2 Percentile evolution of the position error for pulse-to-pulse data and their corresponding skew normal fit sigma's.

Pulse train data	-3σ 0.1per	-2σ 0.2p	-σ 15.9p	mean 50per	σ 84.1p	2σ 97.8p	3σ 99.9p
Total error measurement	0.03	0.04	0.18	0.33	0.59	1.01	1.5
Total error skew fit	0.02	0.04	0.17	0.34	0.6	0.92	1.29
Vertical error raw data	3E-04	0.01	0.07	0.25	0.56	0.98	1.48
Horizontal error raw data	0.01	0.01	0.08	0.16	0.25	0.35	0.47
X error raw data	1E-04	3E-04	0.03	0.11	0.21	0.32	0.41
Y error raw data	1E-04	3E-04	0.03	0.08	0.16	0.28	0.41

6. Other applications

Once the technique is developed, and as the monitoring module is completely independent from the laser system, we can envision various applications, such as the calibration of the scanner system. Indeed, scanners are known for presenting a non-linear response to their input due to the non-linearity of the f-theta lens and need to be calibrated. If the system is not calibrated, when requesting a position on the edge of the processing area, an offset might appear.

With our new monitoring setup, it has become possible to mark a calibration map with the scanner and to automatically obtain the actual laser position without the step with machine vision that is normally used for system calibration. Our test, however, was not done to calibrate our system, but to verify that the calibration that we already had was accurate. To do so, the calibration grid is performed with 21x21 steps of 2.5mm, and we only validate that it is accurate. The map as measured with the multilateration monitoring setup can be seen in Figure 15. With this experiment, we can validate that our setup is correctly calibrated, and that the error measured is within the specification of our monitoring setup.

Another application was done to study the capacity of the system to follow complex 3D structures. To do so, we surface texturized a sport medal with a 2mm heigh drawing of a cup surrounded by a leave crown. A picture of the medal and its height profile as calibrated by an optical profilometer can be visible on Figure 16.

The material of the medal is unknown, which allow us to demonstrate that the system is independent from the process, and we use the same pulse laser system as before to treat the medal surface. A scanning routine was implemented similar to the ones used to remove oxide from metallic samples. In a similar manner, the sound of the interaction between laser and material was recorded by the microphone, and each pulse identified, and the multilateration position calculated. The results obtained are visible on the Figure 17.

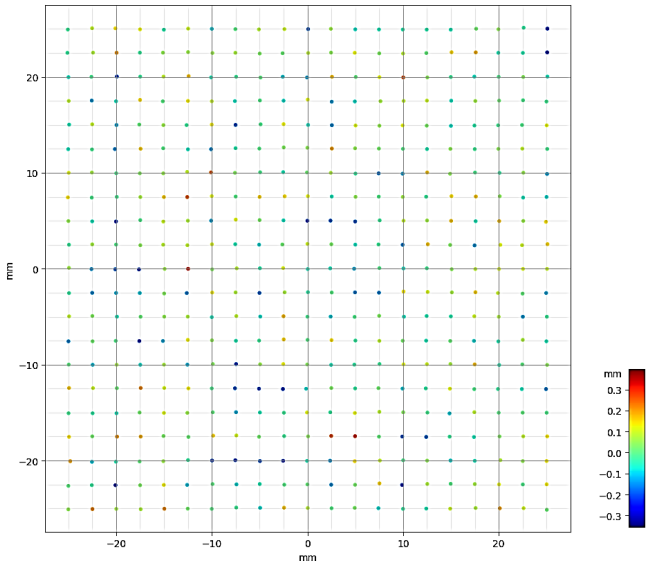

Fig. 15 Results of the calibration verification for our scanner system: each point successfully lands on the grid that we define, and no systematic error is observed on the edges.

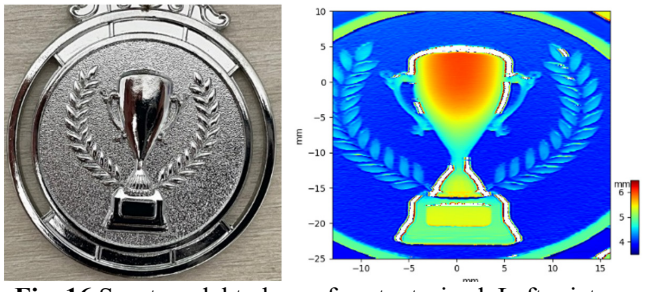

Fig. 16 Sport medal to be surface texturized. Left: picture of the medal. Right: Height of the medal as calibrated with an optical profilometer.

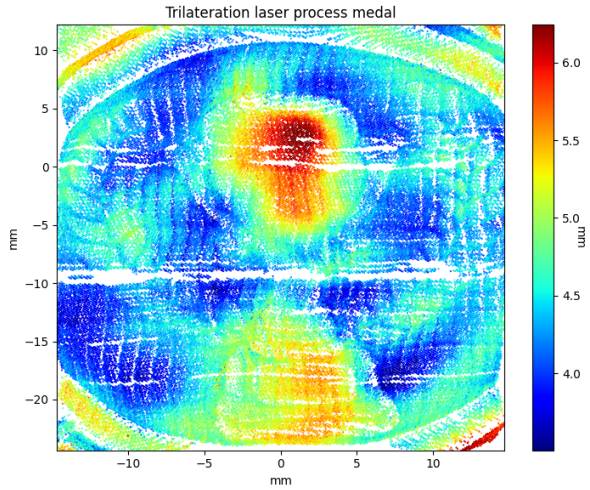

Fig. 17 Results of the multilateration algorithm based on sound capture during the surface cleaning of the medal. Some features are visible, but the results are too noisy to be exploitable.

As we can easily observe, some features appear to be visible, such as the cup or the base of the cup. The leaves also can be visible in some areas. Work is ongoing to improve the accuracy and reliability of the system and to make it more robust.

7. Conclusion and discussion

This study successfully demonstrates the development of a disruptive approach for monitoring laser processes. This innovative method utilizes an array of free-field microphones to pinpoint the spatial position where the laser interacts with the sample through precise Time Difference of Arrival (TDoA) measurements and multilateration algorithms. We have shown that this approach achieves submillimeter accuracy in determining the location of the laser-material interaction. One of the significant advantages of this technique is its complete independence from the laser machine, requiring no input from the setup. Moreover, it is unaffected by process parameters such as laser duration, wavelength, or frequency. As long as the process emits sound, it can be measured and located.

However, this setup does have limitations. Many processes do not produce sufficient acoustic intensity to be captured and analyzed, or they operate at frequencies beyond the capabilities of the microphones used. Higher-performance microphones, such as commercially available free-field piezo microphones that can reach up to hundreds of kHz, or optical microphones capable of reaching the MHz range, could enhance performance.

Additionally, because the sound wave is air-coupled, it is significantly influenced by air blowing and/or suction streams in the process area. Extraction systems can generate winds of up to dozens of meters per second, nearly 10% of the speed of sound, which greatly affects the Time of Flight (TOF) and, consequently, the results of the multilateration algorithm. Potential solutions to these issues include creating a dedicated calibration map and utilizing AI training for position location based on a large number of known acquisitions.

Overall, this study demonstrates the successful implementation of a novel metrology technique for laser surface texturing. Considerable work remains to make this technique robust and mature enough for industrial applications or to adapt the technology for other processes, such as ultrashort lasers, and other applications, including laser welding, cutting, drilling, and other laser-based technologies.

This work was performed within the Bilasurf project, call Horizon-CL4-2022-TwinTransition-01-02, 101091623, and the authors would like to thank the European commission for giving us the opportunity to push research in Europe further.

References

[1] J. Ion: “Laser processing of engineering materials: principles, procedure and industrial application”. (Publisher, Elsevier, 2005) 12.
[2] K. Stanford: “Lasers in metal surface modification”, Metallurgia 47(3), (published, Fuel and Metallurgical Journals., 1980) 109.
[3] S. Marimuthu, S. Pathak, J. Radhakrishnan, and A.M. Kamara: J. Coatings, 11, (2021) 886.
[4] V. Firago, O. Devoino, and A. Lapkovsky: J. Appl. Spectrosc., 89, (2022) 731.
[5] X. Xie, Q. Huang, J. Long, Q. Ren, W. Hu, and S. Liu: J. Mater. Process. Technol., 275 (2020) 116321.
[6] T. Steege, S. Alamri, A. Lasagni, and T. Kunze: Sci. Rep., 11, (2021) 14540.
[7] C. Stauter, P. Gerard, J. Fontaine, and T. Engel: J. Appl. Surf. Sci., 109, (1997) 174.
[8] A. Kacaras, M. Bächle, M. Schwabe, F. Zanger, F. Puente León, and V. Schulze: Procedia CIRP, 81, (2019) 270.
[9] B. T. Fang: IEEE Trans. Aerosp. Electron. Syst., 26, (1990) 748.
[10] S. Niilo: Proc. 2010 7th Workshop on Position., Navig. And Commun., (2010) 38.
[11] S. Bancroft: IEEE Trans. Aerosp. Electron. Syst., 21, (1985) 56.
[12] C. Yiu Tong, K. C. Ho: IEEE Trans. Signal Process, 42, (1994) 1905.
[13] B. T. Fang: J Guidance Control and Dyn., 9, (1986) 715.
[14] I. Todhunter, and J. G. Leathem: “Spherical Trigonometry: for the Use of Colleges And Schools. 5th ed.” (Publisher, London: Macmillan, 1886.) 256.

(Received: June 15, 2024, Accepted: November 17, 2024)